

TITANYL SULPHATE, AN INORGANIC POLYMER: STRUCTURAL STUDIES AND VIBRATIONAL ASSIGNMENT

Lucia Kiyomi Noda^{a,*},, Fabricio Ronil Sensato^a and Norberto Sanches Gonçalves^a^aInstituto de Ciências Ambientais, Químicas e Farmacêuticas, Departamento de Química, Universidade Federal de São Paulo, Campus Diadema, 09972-270 Diadema – SP, Brasil

Recebido em 08/06/2019; aceite em 02/08/2019; publicado na web em 21/10/2019

In this work, anhydrous titanyl sulfate (TiOSO_4) was synthesized and characterized by elemental analyses and vibrational spectroscopy by the first time. In order to verify the stability of the crystallographic structure reported in the literature, an optimization calculation of the unit cell geometry was done with the CRYSTAL17 software, and the agreement with the experimental results was very good. Raman, infrared and far infrared spectra were obtained, the bands having been tentatively assigned, based on literature data for similar systems. Essentially, the spectra exhibit the vibrational modes of the sulfate anion splitted by the low local symmetry along with the bands of the TiO_6 skeleton. The Raman spectra shows two intense bands, tentatively assigned to Ti-O modes.

Keywords: titanyl sulfate; Raman spectroscopy; infrared spectroscopy; solid state ab initio calculation; CRYSTAL17.

INTRODUCTION

Titanyl sulfate, both in its anhydrous and hydrated form, is an interesting substance from the structural point of view due to its three-dimensional polymer structure and also from the technological standpoint. TiOSO_4 is also a source of obtaining the sulfated titanium dioxide, an important catalyst in the field of Heterogeneous Catalysis. One of the ways of obtaining TiOSO_4 consists in the dissolution of the ilmenite (FeTiO_3) by concentrated H_2SO_4 , yielding intermediately a solution of TiO_2 and ferrous sulfate. TiO_2 is obtained by hydrolysis, giving rise to hydrated TiO_2 , which is separated from the solution containing Fe(II). The anhydrous form of TiO_2 is obtained by heat treatment of the hydrated form, according to Hadjiivanov and Klissurski.¹ Due to the fact that the precursor TiOSO_4 already contains sulfate, it is also possible to obtain sulphated titanium oxide by this route, which, being superacid, allows the formation of intermediate species on its surface, which can be studied by electronic and vibrational spectroscopy.^{2,3}

The titanyl ion, with Ti=O double bond, is hardly found in compounds containing this ion in the solid state, according to Grätzel and Rotzinger.⁴ They cited as examples, the complexes $\text{TiO}(\text{porphyrin})$,⁵ $\text{TiO}(\text{phthalocyanine})$,^{6,7} $(\text{R}_4\text{N})_2\text{TiCl}_4\text{O}$,⁸ $\text{TiO}(\text{edtaH}_2)$ (H_2O)⁹ and $[\text{TiOF}_5]^{3-}$,¹⁰ the latter presenting $\nu(\text{Ti}=\text{O})$ wavenumber at ca. 950 cm^{-1} . Some titanyl compounds in aqueous solution have the Ti=O bond, for example, $\text{TiO}(\text{ClO}_4)_2$ in acid medium, with a weak band at 975 cm^{-1} assigned to Ti=O stretching.^{4,11} However, the predominant species are oligomers or protonated species, in which the bonding order is lower.⁴ Titanyl sulfate in the solid state has a polymer chain -Ti-O-Ti-O-Ti-O-, also observed in compounds TiOX_2 (X = F, Cl, Br, I).¹² X-ray diffractograms of TiOSO_4 have provided the most realistic structure, in which the titanium is hexacoordinated.¹³

As will be shown below, the structure presents Ti-O(4)- zigzag chains with short Ti-O(4) bonds, connected by sulfate groups (2 O(1), O(2) and O(3)), the corresponding Ti-O bonds are longer than the Ti-O bonds of the chain. Two possible symmetries were proposed for the space group, Pnma or Pna2₁. Although there are infrared absorption spectroscopy data for the monohydrate and the dihydrate,¹⁴ the literature does not report characterization studies of solid anhydrous

TiOSO_4 by Raman or infrared vibration spectroscopy, which is the main objective of this work.

EXPERIMENTAL

Syntheses

Anhydrous titanyl sulfate (TiOSO_4) was prepared according to the method described by Kjekshus *et al.*¹³ in which 1.6 g of TiO_2 (TIBRAS) is refluxed with 20 mL of concentrated H_2SO_4 (LabSynth) under magnetic stirring for four hours in a 50 mL flask with condenser. At first it is observed dissolution of the TiO_2 , giving rise to a light yellow solution, which slowly becomes cloudy. After cooling, the precipitate is filtered in sintered glass, followed by washing with glacial acetic acid and ethyl ether, followed by drying in vacuum. The material obtained is in the form of a white powder. The sulfur content obtained for TiOSO_4 was 20.50% (expected = 20.01%).

Spectroscopic methods

Infrared absorption spectra were obtained employing the KBr pellet method. KBr was spectroscopic grade from clived windows to assure minimum water content. It was also possible to use absorption spectroscopy in the far infrared region, with the sample dispersed in mineral oil between HDPE plates. The equipments used were a Shimadzu FTIR Prestige-21 fitted with DTGS/KBr detector and Ge@KBr beamsplitter for the mid infrared region and a Bomem DA3.16, equipped with global source, DTGS detector with polyethylene windows and Mylar 3 micra beamsplitter. With these assemblies regions of 4000 to 400 cm^{-1} and from 400 to 100 cm^{-1} were recorded. Raman spectra were recorded on a Renishaw InVia, with the line at 632.8 nm of the He-Ne laser. Laser power was adjusted to 1.5 mW . The sample was placed in a slide glass and slightly pressed. This sample was left in the air for three days and the spectrum was repeated; reproducibility was verified, which demonstrated the stability of the sample against humidity. Spectral resolution was set to 4 cm^{-1} for all spectra.

Computational methods

Our work was supplemented by electronic structure calculations

*e-mail: lucia.noda@unifesp.br

at DFT level, which were performed using the computer code CRYSTAL17.¹⁵ For the exchange-correlation (XC) potential it was applied the revised PBE generalized gradient approximation for solids, PBEsol.¹⁶ CRYSTAL17 uses a local Gaussian basis set, as opposite to the plane waves that are the most common choice in quantum programs devoted to the solid state. In this work, all-electron basis sets have been employed in the calculations with 86-41131 (one *s*, four *sp* and 2 *d* shell)¹⁷ 86-311111 (one *s*, five *sp* and two *d* shell)¹⁸ and 8-4111 (one *s*, three *sp* and one *d* shell)¹⁹ contractions for titanium, sulfur and oxygen atoms, respectively. All of them are available via the online library of the code.²⁰ We employed a Monkhorst–Pack shrinking factor of 8 for reciprocal space sampling. The calculations were conducted using Coulombic and exchange integral tolerance factors of 6, 6, 6, 6 and 12 (TOLINTEG) and the accuracy on the SCF convergence (TOLDEE) was set to 10. The crystal structure has been optimized by minimizing the total energy with respect to the lattice parameters and the position of atoms in the unit cell.

RESULTS AND DISCUSSION

Computational Methods

In particular, the crystallographic structure of TiOSO_4 is orthorhombic with the space group Pnma , number 62 in the standard listing. The primitive cell contains four TiOSO_4 formula units, $Z=4$. Yet, there are five non-equivalent atoms in the corresponding asymmetric unit, namely, Ti, S, O(1), O(2), O(3) and O(4).¹³ A Moldraw^{21,22} representation of the TiOSO_4 structure, as well as the labeling scheme for the non-equivalent atoms are depicted in Figure 1. Such a representation provide a side-on view of the infinite $-\text{Ti}-\text{O}-$ zigzag chains along the *b*-direction, which is a very distinctive feature of this structure.

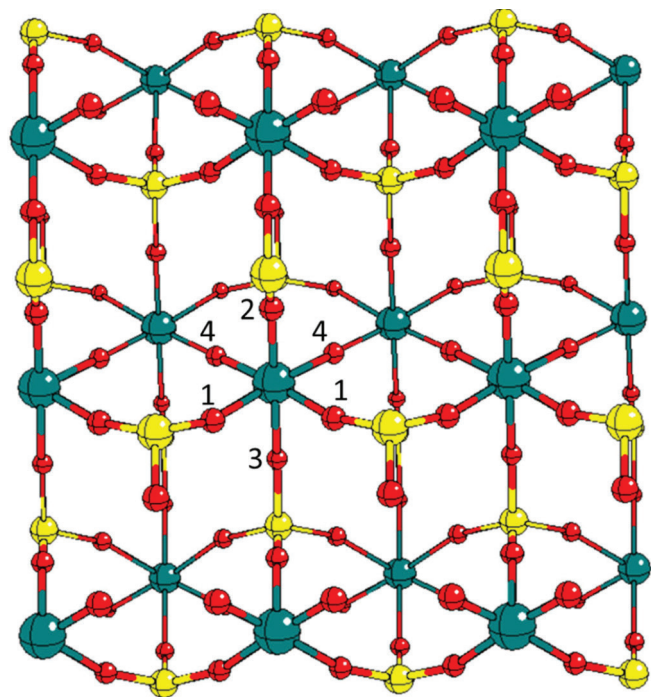


Figure 1. Crystallographic structure of the titanium oxide sulfate TiOSO_4 viewed down the *c* axis, showing atom numbering. Green, red and yellow spheres represent the Ti, O e S atoms, respectively

Optimizations were carried out starting from experimental data given by Ahmed and co-workers.¹³ The optimized parameters

for TiOSO_4 bulk are as follow: $a = 11.160 \text{ \AA}$, $b = 5.264 \text{ \AA}$ and $c = 6.607 \text{ \AA}$, which are in good agreement with experimental data, namely, 10.953 \AA , 5.152 \AA and 6.426 \AA , respectively. The main bonding distances are presented in Table 1. Both the titanium and sulfur atoms are at sites 4c (corresponding to the Wickof notation reflection operation) according to Ahmed *et al.*¹³ The calculation did not alter these local symmetries.

Table 1. Calculated interatomic distances, in Å , for the crystal structure of TiOSO_4

	Calc.	Exp. ¹³		Calc.	Exp. ¹³
Ti–O(1) × 2	2.095	2.014	S–O(4) × 2	1.489	1.474
Ti–O(2)	1.964	1.876	S–O(2)	1.506	1.496
Ti–O(3)	1.986	1.944	S–O(3)	1.506	1.443
Ti–O(4) × 2	1.789	1.786			

Vibrational Spectroscopy

Figure 2 shows the Raman and infrared spectra for TiOSO_4 .

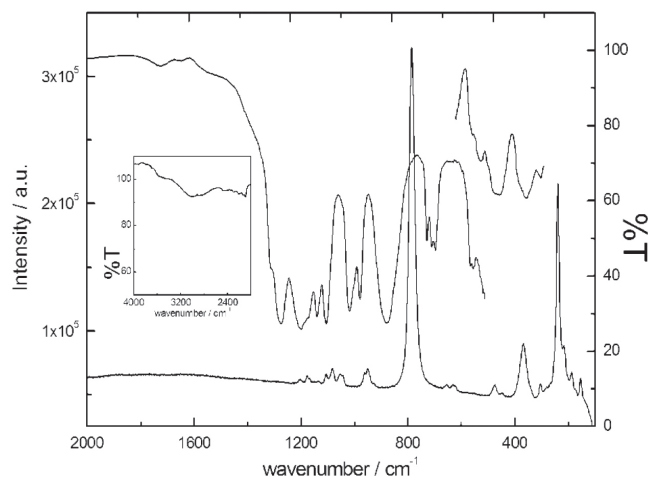


Figure 2. Infrared, far infrared and Raman spectra (632,8 nm) of solid TiOSO_4

From the Raman and IR spectra, it is observed that there is practically no coincidence of bands, indicating the presence of symmetry center, as indicated by the crystallographic data and confirmed by the calculation of the structure. The extensive splitting of sulfate bands indicates a lower symmetry than that of the free sulfate, due to the coordination with the titanium ion, as well as due to the lower local symmetry where the sulfate anion is found. In this case, the sulfate anion occupies a position (4c), which corresponds to the presence of a plane of symmetry. This low symmetry causes the splitting of all sulfate degenerate modes. The correlation and the factor group methods can be invoked to explain the high number of observed bands, since the number of sub-units in the unit cell ($Z = 4$) produce several combinations of normal modes inside the unit cell. The Raman spectrum is quite peculiar, showing two intense bands at 239 and 785 cm^{-1} , in addition to a weaker band at 368 cm^{-1} , the other bands being quite weak. No Raman bands are observed in the 1600 cm^{-1} region, indicating water absence.

The general appearance resembles the Raman spectrum of a coordinated sulfate anion, with several splitted modes, plus bands that may be tentatively assigned to the $[\text{TiO}_6]$ backbone modes. It is important to point out that a reasonable interpretation model should be based on the vibrational modes of both $[\text{TiO}_6]$ and $[\text{SO}_4^{2-}]$ moieties. The expected vibrational representation for octahedral $[\text{TiO}_6]$ is $\Gamma = A_{1g}$

(Raman, stretching) + E_g (Raman, stretching) + T_{1u} (IR, stretching) + T_{1u} (IR, bending) + T_{2g} (Raman, bending) + T_{2u} (inactive, bending); disregarding the splittings, it would be expected three Raman and two infrared bands. Bendings are expected below 400 cm^{-1} and stretchings, above 400 cm^{-1} . For the $[\text{SO}_4^{2-}]$ group, is expected the usual pattern for a tetrahedral XO_4 , for instance, $\Gamma = A_1$ (Raman, stretching) + E (Raman, bending) + T_2 (IR, stretching) + T_2 (IR, bending).

Table 2 shows the experimental infrared and Raman wavenumbers.

Table 2. Experimental infrared and Raman wavenumbers (cm^{-1}), with tentative assignment (see text), for TiOSO_4

IR	Raman	Assignment
	154(w)	
	187(w)	lattice modes
211(vw)		
	239(s)	
269(m)		
295(sh)		
	304(vw)	
	368(m)	δ TiO_6 modes
373(m)		
387(m)		
418(sh)		
446(w)		
	474(vw)	
478(w)		ν_2 (SO_4^{2-})
490(w)		
	628(vw)	
629(m)		
642(m)		ν_4 (SO_4^{2-})
	654(vw)	
661(m)		
	785(vs)	ν (Ti-O)s
819(s,br)		ν (Ti-O)
925(m)		
	949(w)	
	961(w)	ν_1 (SO_4^{2-})
967(s)		
	1044(w)	
	1053(w)	
1059(m)		
	1081(w)	
1094(m)		
	1105(w)	
	1134(vw)	ν_3 (SO_4^{2-})
1129(sh)		
1156(m)		
	1169(vw)	
	1176(wv)	
	1203(vw)	
1236(m)		
1277(sh)		
1715 (vw)		
2092(w)		
2131(vw)		combination bands
2209(w)		
2467(vw)		
2966(w,br)		adsorbed water

In order to find out which bands in the Raman spectrum should be assigned to the $[\text{TiO}_6]$ skeleton, it is enough to identify the ones due to the $[\text{SO}_4^{2-}]$ group, whose wavenumber modes do not vary significantly, when compared with other compounds containing this anion. The remaining bands can then be assigned to the $[\text{TiO}_6]$ moiety. However, it should be remembered that lattice modes involving translations and librations of the $[\text{SO}_4^{2-}]$ and $[\text{TiO}_6]$ groups are expected in the low wavenumber region. The band at 368 cm^{-1} is in the borderline between lattice and $[\text{TiO}_6]$ angular deformation modes. The intense band at 785 cm^{-1} was tentatively assigned to totally symmetric stretching mode of this group. Such an assignment takes into account the following arguments: (i) the high intensity of this band should be probably due to metal-oxygen bond higher polarizability and its totally symmetric nature; (ii) the observed wavenumber value is close to that reported for other compounds containing Ti-O bonding, with a bond order less than 2.^{23,24} In the infrared spectrum, the band at 819 cm^{-1} is also tentatively assigned to a ν (Ti-O) stretching mode. The medium bands at 925 and 967 cm^{-1} in the infrared spectra, as well as the weak Raman bands at 949 and 961 cm^{-1} , although initially assignable to $\nu_1(\text{SO}_4^{2-})$, may have some contribution from ν (Ti-O) stretching modes.²⁵ The justification for this would be as follows. In some compounds, where the titanium ion is connected to a single oxygen atom, forming a true Ti=O bond, a single vibrational mode is expected, occurring at highest wavenumbers, near 950 cm^{-1} .^{4,11} In the TiOSO_4 crystal structure, there is a short Ti-O bond (Ti-O(4), 1.786 \AA), whose character may be considered to be intermediate between a single and a double bond [compare with 1.62 \AA for TiO(porphyrin)].⁵ Assuming these Ti-O bonds behave as individual oscillators, bands with a wavenumber greater than 900 cm^{-1} could be assigned to ν (Ti-O) stretching modes involving shorter Ti-O bonds, such as the Ti-O(4) bond. Moreover, another argument to consider is the fact that the oxygen atom of this shorter Ti-O(4) bond is just that belonging to the $[\text{SO}_4^{2-}]$ group. Thus, the presence of a mechanical coupling between the ν (Ti-O) stretching involving the Ti-O(4) bond and the $\nu_1(\text{SO}_4^{2-})$ may be considered. These arguments justify the presence of some ν (Ti-O) character in the vibrational modes assigned to $\nu_1(\text{SO}_4^{2-})$; this could explain the relatively high intensity observed in the infrared spectra for ν_1 totally symmetric mode together with reduced local symmetry effects that make it infrared active. However, an exact and quantitative description of the normal modes requires a normal coordinate calculation, either by the classical or by ab initio methods; this problem is currently being investigated in our group using the CRYSTAL17 capabilities. Preliminary results indicate extensive normal mode mixing involving the two moieties.

Similarly to the Raman spectrum, the infrared spectrum essentially shows the splitted $[\text{SO}_4^{2-}]$ group modes, with, as already mentioned, an extra band at 819 cm^{-1} , assigned to a ν (Ti-O) stretching mode. It should be remembered that this value is lower than that observed in titanium compounds with Ti=O double bond (ca. 950 cm^{-1}). The splitting pattern resembles that of the sulfated TiO_2 ,²⁶⁻²⁸ mainly in the $\nu_4(\text{SO}_4^{2-})$ region, in the range of 1050 to 1200 cm^{-1} . An important evidence that the compound analyzed is really the anhydrous TiOSO_4 is the absence of the angular deformation mode of water at ca. 1600 cm^{-1} , as was also observed in the Raman spectrum. However, there is a weak and broad band seen at 2966 cm^{-1} . It has a somewhat low wavenumber to be assigned to adsorbed water; the presence of some reticular water should be considered. The low wavenumber may indicate a very intense hydrogen bond. In this situation, there is usually a large increase in intensity due to increased anharmonicity. In this way, despite the apparent intensity, the amount of water must be small. The bands in the 2000 - 2500 cm^{-1} can be assigned to combination or harmonic bands. Another important point is that the number of expected modes (from correlation or factor group method)

is usually much higher than the observed ones, which is certainly due to low-intensity modes and accidental degeneracy.

CONCLUSIONS

From the experimental Raman and infrared spectra, it was possible to verify that mutual Raman/infrared exclusion rule is operative and allows confirming that the crystalline structure is centrosymmetric, which favors Pnma symmetry, instead of Pna2₁. Strong Raman bands were assigned to lattice modes and $\nu_s(\text{Ti-O})$. The geometry optimization calculations employing CRYSTAL17 were satisfactory, taking into account the calculated/experimental concordance. This seeds the basis for additional calculations involving vibrational wavenumbers, which will be useful for confirming the proposed assignment.

ACKNOWLEDGEMENTS

The authors are grateful to LEM (IQUSP, São Paulo) for the far infrared spectra on Bomem DA3.16 and to FAPESP (process 2017/06194-2) for the financial support.

REFERENCES

- Hadjiivanov, K. I.; Klissurski, D. G.; *Chem. Soc. Rev.* **1996**, 25, 61.
- Noda, L. K.; Rosales, R.; Gonçalves, N. S.; Sala, O.; *J. Raman Spectrosc.* **2008**, 39, 415.
- Gonçalves, N. S.; Rettori, D., Silva, G. M. G., Noda, L. K.; *Vib. Spectrosc.* **2018**, 99, 80.
- Gratzel, M.; Rotzinger, F. P.; *Inorg. Chem.* **1985**, 24, 2320.
- Dwyer, P. N.; Puppe, L.; Buchler, J. W.; Scheidt, W. R.; *Inorg. Chem.* **1975**, 14, 1782.
- Taube, R.; *Z. Chem.* **1963**, 3, 194.
- Block, B. P.; Meloni, E. G.; *Inorg. Chem.* **1965**, 4, 111.
- Feltz, A.; *Z. Chem.* **1967**, 7, 158.
- Kristine, F. J.; Shepherd, R. E.; Siddiqui, S.; *Inorg. Chem.* **1981**, 20, 257.
- Dehnicke, K.; Pausewang, G.; Rüdorff, W.; *Z. Anorg. Allg. Chem.* **1969**, 366, 64.
- Comba, P.; Merbach, A.; *Inorg. Chem.* **1987**, 26, 1315.
- Clark, R. J. H.; Bradley, D. C.; Thornton P.; *Pergamon Texts in Inorganic Chemistry* **1973**, 19, 377.
- Ahmed, M. A. K.; Fjellvag, H.; Kjekshus, A.; *Acta Chem. Scand.* **1996**, 50, 275.
- Reynolds, M. L.; Wiseman, T. J.; *J. Inorg. Nucl. Chem.* **1967**, 29, 1381.
- Dovesi, R.; Erba, A.; Orlando, R.; Zicovich-Wilson, C. M.; Civalieri, B.; Maschio, L.; Rerat, M.; Casassa, S.; Baima, J.; Salustro, S.; Kirtman, B.; *Wiley Interdiscip. Rev.: Comput. Mol. Sci.* **2018**, 8, e1360.
- Perdew, J. P.; Ruzsinszky, A.; Csonka, G. I.; Vydrov, O. A.; Scuseria, G. E.; Constantin, L. A.; Zhou, X. L.; Burke, K.; *Phys. Rev. Lett.* **2008**, 100, 136406.
- Mackrodt, W. C.; Simson, E. A.; Harrison, N. M.; *Surf. Sci.* **1997**, 384, 192.
- Bredow, T.; Heitjans, P.; Wilkening, M.; *Phys. Rev. B* **2004**, 70, 115111.
- Cora, F.; *Mol. Phys.* **2005**, 103, 2483.
- <http://www.crystal.unito.it/basis-sets.php>, accessed September 2019.
- Ugliengo, P.; *MOLDRAW: A program to display and manipulate molecular and crystal structures*, Torino, 2006, available at <http://www.moldraw.unito.it>.
- Ugliengo, P.; Viterbo, D.; Chiari, G.; *Z. Kristallogr.* **1993**, 207, 9.
- van de Velde, G. M. H.; Harkema, S.; Gellings, P. J.; *Inorg. Nucl. Chem. Lett.* **1973**, 9, 1169.
- Barracough, C. G.; Lewis, J.; Nyholm, R. S.; *J. Chem. Soc.* **1959**, 3552.
- Bragina, M. I.; Tsevtkova, M. P.; Bobyrenko, Y. Y.; *Rus. J. Phys. Chem.* **1977**, 51, 720.
- Noda, L. K.; de Almeida, R. M.; Gonçalves, N. S.; Probst, L. F. D.; Sala, O.; *Catal. Today* **2003**, 85, 69.
- Noda, L. K.; de Almeida, R. M.; Probst, L. F. D.; Gonçalves, N. S.; *J. Mol. Catal. A: Chem.* **2005**, 225, 39.
- de Almeida, R. M.; Noda, L. K.; Gonçalves, N. S.; Meneghetti, S. M. P.; Meneghetti, M. R.; *Appl. Catal., A* **2008**, 347, 100.

FAPESP helped in meeting the publication costs of the article